

# Broadening of the transition between charge states in the single-electron box by the measurement process

Roland Schäfer,\* Bernhard Limbach,† Peter vom Stein,† and Christoph Wallisser  
*Forschungszentrum Karlsruhe, Institut für Festkörperphysik, Postfach 3640, 76021 Karlsruhe, Germany*  
 (Dated: November 17, 2018)

We report on measurements on a sample consisting of two nominally identical single-electron transistors the islands of which are coupled capacitively. One transistor at a time is operated as electron box. The remaining transistor is used as an electrometer to measure the charge on the box island. While ramping up the box gate voltage transitions occur periodically between states which differ in the charge on the box island by the elementary charge  $e$ . This shows up in jumps of the electrometer current. The coupling between the box and the measuring device causes a broadening of the transition width not included in the formulae for an isolated box. This is evident in our data as well as from a thorough analysis of the system in the framework of the sequential tunneling model.

PACS numbers: 73.23.Hk, 85.35.Gv, 73.63.Rt

The most sensitive electrometer known today can be built by utilizing single-electron effects. This has been clearly demonstrated for the first time in the early Nineties by experiments of the Saclay group (e.g. Ref. 1) where a single-electron transistor was used to read out the charge state of a single-electron box with an accuracy of about  $10^{-4}e$ . In principle one can imagine a huge variety of applications of such a sensitive device in solid state science. Nevertheless, the use of single-electron transistors to detect fractions of an elementary charge has not become an everyday standard yet, mainly due to the stringent experimental demands. To build single-electron devices, micro-structuring facilities are needed which are as yet on the leading edge of modern technology. Even with this technology at hand one is restricted to low temperatures (typically below 1 K) and to samples where the electrometer and the device under test are integrated in close vicinity on a joint substrate. Recently the single-electron electrometer has gained new attention as it might serve as a detector of the coherent state of a qubit represented by a superconducting charge box [2, 3]. As already apparent from these works a detailed understanding of the coupling between the single-electron transistor and a charge box and the repercussions of the measurement process on the charge state is highly desirable.

This letter contributes two fold. Primarily we present measurements of the charge-state transition width for a normal-conducting sample consisting of two single-electron transistors which are capacitively coupled in a layout very similar to the one used in Ref. 1. Each of the transistors can be operated as single-electron box by connecting source as well as drain to ground. The average number of electrons on the island of this device is a step-like function of the gate voltage, with the step height corresponding to one electron. The remaining transistor is operated as an electrometer by applying a source-to-drain voltage  $V_{sd}$  slightly above the threshold of the

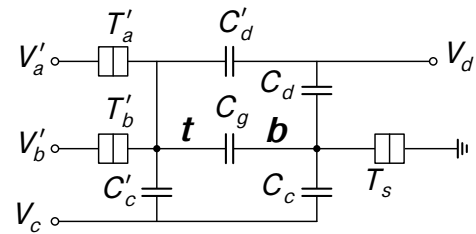


FIG. 1: Transistor  $t$  and box  $b$  coupled by the capacity  $C_g$ . Tunnel contacts  $T$  are characterized by a capacity  $C$  and a conductance  $G$  where the proper indexing is indicated in the figure. The tunnel contact  $T_s$  is built from two contacts in parallel, namely  $T_a$  and  $T_b$ .

Coulomb blockade. Then the step-like behavior shows up in a saw-tooth like variation of the transistor current. For instance, Bouchiat et al. [4] reported that the step-like behavior can be well described by

$$f(m_b) = 1 / (1 + \exp(\beta E_b(1 - 2m_b))), \quad (1)$$

where we have introduced the dimensionless gate charge  $m_b = V_g C_g / e$ ,  $C_g$  being the box-gate capacitance, and denote the charging energy of the box by  $E_b$ . Thus if the charging energy of the box is known, an inverse effective temperature  $\beta_{\text{eff}} = 1 / (k_B T_{\text{eff}})$  can be extracted from the measurements and compared to the temperature of the heat bath the sample is coupled to. In Ref. 4 a fairly good agreement between  $\beta_{\text{eff}}$  and the bath temperature was found and the linear dependence of  $(\beta_{\text{eff}} E_b)^{-1}$  on  $T$  has actually been used to extract the charging energy  $E_b$ . Below we present strong evidence that in general the measurement of the box-charge state by means of a capacitively coupled electrometer leads to a back action onto the charge state itself and as a consequence to a broadening of the transition width which is not accounted for by the simple dependence given above. This evidence is contained in our experimental data. As the second goal of this letter we present an analysis of the complete

system consisting of the box and the electrometer in the framework of the sequential tunneling approach [5]. This approach allows for identifying one simple process which by means of back action leads to a broadening of the charge-state transition width.

In the description of the most relevant properties of the system we restrict ourselves to the so called sequential model which is known to describe systems of small tunnel junctions with conductances  $G$  small compared to  $G_K = e^2/h$  to lowest order in  $g = G/G_K$ . The system of interest is sketched in Fig. 1. The total charge on the box and transistor island is given by  $Q_b = U_b C_b - em_b - U_t C_g$  and  $Q_t = U_t C_t - en_t - U_b C_g$ , respectively. Here  $U_b$  and  $U_t$  are the electrical potential on the box and transistor island,  $em_b = V_c C_c + V_d C_d$  and  $en_t = V_c C'_c + V_d C'_d + V'_a C'_a + V'_b C'_b$  are the negative box and transistor island charge at  $U_b = U_t = 0$ , respectively, and we defined  $C_b = C_c + C_d + C_g + C_s$  and  $C_t = C'_a + C'_b + C'_c + C'_d + C_g$ . In the experiment  $C_d$  and  $C'_c$  represent the primary gates of the box and the transistor, respectively, while  $C_c$  and  $C'_d$  are considerably smaller and represent the unavoidable stray capacitances. The relations for  $Q_b$  and  $Q_t$  yield  $eU_b = 2E_b(Q_b/e + m_b) + 2E_g(Q_t/e + n_t)$  and  $eU_t = 2E_t(Q_t/e + n_t) + 2E_g(Q_b/e + m_b)$ , where we have introduced  $2E_b = e^2/(C_b - C_g^2/C_t)$ ,  $2E_t = e^2/(C_t - C_g^2/C_b)$  and  $2E_g = e^2 C_g/(C_b C_t - C_g^2)$ . In the sequential model the states of the system are classified by the number of excess electrons on the box and transistor island,  $m$  and  $n$ , respectively. The total charging energy of the system depends on the dimensionless polarization charges  $m_b$  and  $n_t$  as well as on  $m$  and  $n$  and may be evaluated from  $E_{(m,n)}(m_b, n_t) = \int_{-em_b}^{-em} U_b(Q_t = -en_t) dQ_b + \int_{-en_t}^{-en} U_t(Q_b = -em) dQ_t$ :

$$E_{(m,n)}(m_b, n_t) = E_b(m - m_b)^2 + E_t(n - n_t)^2 + 2E_g(m - m_b)(n - n_t) \quad (1)$$

Transitions between the states occur via tunneling of electrons across the tunneling barriers. Tunneling across  $T'_a$  and  $T'_b$  onto the transistor island is associated with an energy consumption of  $\Delta E_i(n) = \int_{-ne}^{-(n+1)e} (U_t - V'_i) dQ_t = 2E_t(n + 1/2 - n_t) + 2E_g(m - m_b) + eV'_i$ ,  $i \in \{a, b\}$ . These tunneling events mediate between states differing in  $n$  by one. Similarly  $\Delta E_s(m) = \int_{-me}^{-(m+1)e} U_b dQ_b = 2E_b(m + 1/2 - m_b) + 2E_g(n - n_t)$  describes tunneling across  $T_s$  mediating between states differing in  $m$  by one. Tunneling rates for the individual junctions can be deduced using Fermi's golden rule [5]:  $\Gamma_i(k \rightarrow k+1) = (g_i/h)\Delta E_i/(\exp(\beta\Delta E_i) - 1)$ ,  $i \in \{a, b, s\}$ . Here  $g_i$  is the dimensionless conductance  $g_i = G_i/G_K$ , of the corresponding contact,  $k$  has to be identified with  $m$  if  $i = s$  or with  $n$  otherwise. The inverse processes of tunneling from the islands to the leads is associated with an energy of the same magnitude but opposite sign. The

master equation for the occupation probabilities of the states  $(m, n)$  reads:

$$\begin{aligned} \dot{p}_{(m,n)} &= (\Gamma_a(n_+ \rightarrow n) + \Gamma_b(n_+ \rightarrow n))p_{(m,n_+)} + \\ &(\Gamma_a(n_- \rightarrow n) + \Gamma_b(n_- \rightarrow n))p_{(m,n_-)} + \\ &\Gamma_s(m_+ \rightarrow m)p_{(m_+,n)} + \Gamma_s(m_- \rightarrow m)p_{(m_-,n)} \\ &- (\Gamma_a(n \rightarrow n_+) + \Gamma_b(n \rightarrow n_+) + \\ &\Gamma_a(n \rightarrow n_-) + \Gamma_b(n \rightarrow n_-) + \\ &\Gamma_s(m \rightarrow m_+) + \Gamma_s(m \rightarrow m_-))p_{(m,n)} \\ &= 0, \end{aligned} \quad (2)$$

where the last equality explicitly states that one looks for stationary solutions and  $k_{\pm}$  is a shorthand for  $k \pm 1$ . The physical quantities which matter in the framework of this letter are the mean box charge  $\bar{m} = \sum_{m,n} m p_{(m,n)}$  and the transistor current  $I_{sd} = \sum_{m,n} -e(\Gamma_a(n \rightarrow n+1) - \Gamma_a(n \rightarrow n-1))p_{(m,n)}$ . For given  $n_t$  and  $m_b$  only a limited number of states have to be taken into account, as Eq. (2) in conjunction with Eq. (1) describes an exponentially small occupation probability for states  $(m, n)$  with  $E_{(m,n)}(m_b, n_t) \gg \beta^{-1}$ . Furthermore we can restrict ourselves to the range  $-0.5 \leq m_b \leq 0.5$  and  $0 \leq n_t \leq 1$ , as larger variations in  $m_b$  and  $n_t$  can be incorporated in successive readjustments of  $m \rightarrow m \pm 1$  and  $n \rightarrow n \pm 1$  each time  $n_t$  or  $m_b$  have changed by more than unity, as apparent from (1). At low temperatures it therefore turns out that one has to consider the occupation of six states only. At  $m_b = 0$  only states  $(m, n)$  with  $m = 0$  are occupied with considerable probability. On changing  $m_b$  towards  $m_b = 1$  the probability is successively shifted to states  $(m, n)$  with  $m = 1$ . The current  $I_t$  in the transistor at  $n_t \in [-0.5, 0.5]$  and at source-to-drain voltages  $V'_a - V'_b \lesssim 2E_t/e$  is dominantly sustained by states  $(m, n)$  with  $n \in \{-1, 0, 1\}$ . Taking only six states into account Eq. (2) takes the form  $\sum_j M_{ij} p_j = 0$  where  $i, j \in \{(0, 0), (0, 1), (1, 1), (1, 0), (1, -1), (0, -1)\}$ . The one-dimensional null-space of the matrix  $M_{ij}$  is most easily found with modern computer algebra systems. So we will do without writing down the lengthy expressions for  $p_i$  here. At elevated temperature more states are involved and we have to fall back upon numerical methods in solving Eq. (2). In this case after an initial guess for the probabilities  $p_{(n,m)}$  the time evolution described by the master Eq. (2) is used in an iterative relaxation procedure which in general converges towards a stationary solution.

Our sample is fabricated by standard e-beam lithography in conjunction with a shadow evaporation technique from aluminum with aluminum-oxide barriers. The sample parameters can be found by analyzing the behavior of the transistor's current at high  $V_{sd}$  ( $E_c$ ,  $E'_c$  and the tunnel conductances are determined this way) and from various periods seen in Coulomb oscillation measurements:  $E_c = 2.03 \pm 0.05 k_B K$ ,  $E'_c = 1.93 \pm 0.05 k_B K$ ,  $E_g = 0.112 \pm 0.009 k_B K$ ,  $C_d = 69$  aF,  $C'_c = 66$  aF,

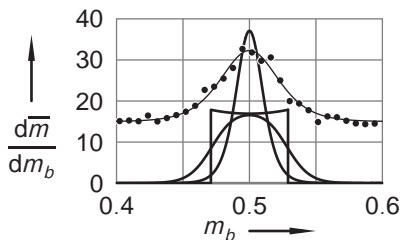


FIG. 2: The derivative of the mean box charge with respect to  $m_b$  as a function of  $m_b$  as calculated from the six state approximation (thick lines). Highest peak:  $n_t = 0$  and  $k_B T = 0.0135 E_b$  ( $\sim 26$  mK). Curve with discontinuities:  $n_t = 0.5$  and  $T = 0$ . Broad curve:  $n_t = 0.5$  and  $k_B T = 0.0135 E_b$ . The dots are taken from a measurement at 26 mK normalized to yield a unity integral, and offset for clarity. Thin line: Best fit of Eq. (1') to the experimental data corresponding to  $T_{\text{eff}} = 56$  mK.

$C_c = 23.2$  aF,  $C'_d = 20.8$  aF,  $g_a \sim g_b = 0.120 \pm 0.002$ , and  $g'_a \sim g'_b = 0.130 \pm 0.002$ .

The measurements are performed in the mixing chamber of a top-loading dilution refrigerator. The details of the experimental setup are described elsewhere [6]. During each measurement one of the transistors is operated as single-electron box while the other one is used as electrometer. The working point of the latter is selected by applying a voltage  $V_{\text{sd}}$  slightly above the threshold of the coulomb blockade  $V_{\text{sd}} \gtrsim 2E_t/e$  and choosing a constant  $n_t$ . To gain resolution a lock-in technique has been used. The mean value of  $m_b$  which is varied slowly with a rate of about  $0.2 \text{ min}^{-1}$  is superimposed by an AC signal of small amplitude with a frequency of 34.15 Hz. The AC component of the current response is detected by a lock-in amplifier. This signal is to a good approximation proportional to the derivative of the current  $dI_{\text{sd}}/dm_b$ . The derivative has peaks where jumps in the current signal the transition of the box charge between neighboring states. The width of the peaks may be related to an effective temperature  $T_{\text{eff}}$  by comparing it to the ideal behavior of a single-electron box. To do so the measured curves are fitted to a function of the form  $h(m_b) = c f'(m_b) + d$ , where  $c$  accounts for the sensitivity by which variations of the box charge are transferred to variations of the electrometer current via the coupling capacity  $C_g$ . Similarly,  $d$  accounts for the fact that the step-like change of the box charge is transferred to a saw-tooth like current variation by adding an appropriate tilt  $dm_b$ . Finally

$$f(m_b) = \sum_m m \exp(-\beta_{\text{eff}} E_m) / \sum_m \exp(-\beta_{\text{eff}} E_m) \quad (1')$$

is the step function of the single-electron box not coupled to any measuring device. Note that Eq. (1) is a low temperature approximation of Eq. (1'). Here  $E_m = E_b(m - m_b)^2$  is the electrostatic energy of the box island charged by  $m$  electrons. In Fig. 2 a part of a measurement is shown together with the least-squares fit

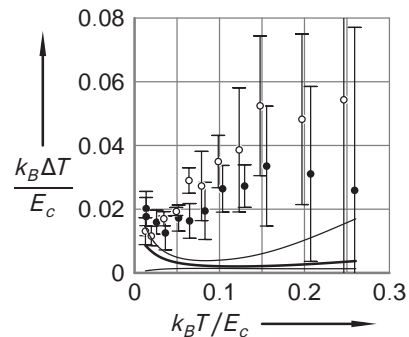


FIG. 3:  $\Delta T = T_{\text{eff}} - T$  as a function of  $T$ . Closed circles: Configuration with  $E_b = 1.93 k_B K$ . Open Circles: Configuration with  $E_b = 2.03 k_B K$ . Lines: result for the sequential model (see text).

of  $h(m_b)$  to these data. Measurements have been taken in the temperature range from 26 mK, the lowest temperature we could reach, up to 500 mK. With increasing temperature the peaks in  $dI_{\text{sd}}/dm_b$  get wider and their amplitude decreases. Above 500 mK the signal gets buried in the experimental noise.

Fig. 3 summarizes our main finding. At each temperature we took measurements of  $dI_{\text{sd}}/dm_b$  at up to 100 different values of  $n_t$ . By varying  $n_t$  we change the working point of the electrometer. At  $n_t = 0$  and  $n_t = 0.5$  the electrometer current takes its minimal and maximal value for a given source-to-drain voltage. At these points the electrometer has no sensitivity; small changes of the box charge do not result in a variation of the electrometer current. In between the electrometer's sensitivity is finite. Of all measurements taken we selected those for a further analysis where a periodic peak structure is clearly visible. For these measurements the parameter  $T_{\text{eff}}$  is determined. The difference between the mean of  $T_{\text{eff}}$  and the temperature  $T$  in the mixing chamber of our dilution refrigerator is depicted as dots in Fig. 3 while the root mean square deviation from the mean value is indicated by the error bars. The effective temperature  $T_{\text{eff}}$  lies significantly above the temperature of the heat bath in which the sample is immersed. In principle this could have several reasons. One may argue that our single-electron box is not in thermal equilibrium with the heat bath or that a small fraction of black body radiation from parts of the experimental equipment which is at higher temperatures than the sample itself enters the metallic cavity containing the sample and spoils the experimental results by triggering photo-assisted tunneling events. However, even though it is almost impossible to rule out pollution effects with certainty, their signature is in general different from our findings. Usually those effects are less important at elevated temperature and cause the saturation of certain physical quantities below some threshold indicating that cooling the system by further decreasing the temperature of the heat bath

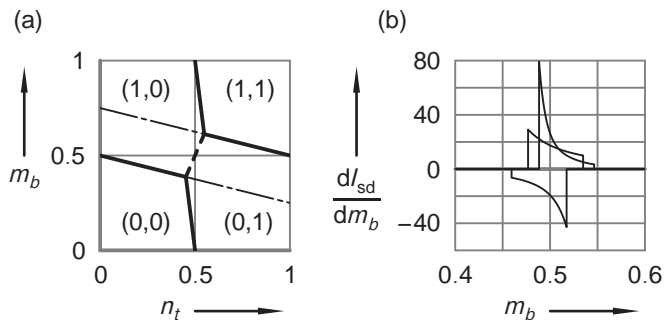


FIG. 4: (a): Stability diagram for the system at zero  $V_{sd}$  for  $E_t/E_b = 2$  and  $E_b/E_g = 4$ . Thick lines separate regions where certain states  $(m, n)$  have the lowest electrostatic energy. A direct transition between state  $(1, 0)$  and state  $(0, 1)$  across the dashed line is possible only via a higher order process. The thin dot-dashed lines are explained in the text. (b): The derivative of the electrometer current with respect to  $m_b$  as a function of  $m_b$  at zero temperature for different values of  $n_t$  ( $n_t \in \{0.2, 0.4, 0.7\}$ ) from top to bottom) as calculated from the six states approximation. The curves have been normalized to give a total area of unity.

gets inefficient. In our case we find an ongoing decrease of  $T_{\text{eff}}$  to the lowest bath temperatures available. Yet in the whole temperature range  $T_{\text{eff}}$  exceeds the bath temperature significantly.

Further evidence that the enhancement of  $T_{\text{eff}}$  above the bath temperature is an intrinsic effect is gained by analyzing the sequential model. In qualitative agreement with our experimental data it yields a broadening of the width of the transition between neighboring charge states in the box which might be described by an enhanced  $T_{\text{eff}}$ . Fig. 4a shows the stability diagram of the system depicted in Fig. 1 for  $V'_a = V'_b = 0$ . The tilt of the thick lines and the occurrence of the dashed line are due to the coupling; without coupling,  $E_g = 0$ , the thick lines would be exactly horizontal and vertical. At finite  $V_{sd} = V'_a - V'_b$  each of the almost vertical lines which correspond to  $\Delta E_a(n) = \Delta E_b(n) = 0$  has to be replaced by two lines whose distance increases with  $V_{sd}$ . On the other hand, the borders between neighboring *box* states stay sharp at zero temperature. The border between state  $(0, 0)$  and  $(1, 0)$  is described by  $m_b = 0.5 - (E_g/E_b)n_t$ . In Fig. 4a it is extended by a thin dot-dashed line to  $n_t = 1$ ; this line we name border I. For the border between state  $(0, 1)$  and  $(1, 1)$  the relation  $m_b = 0.5 + E_g/E_b(1 - n_t)$  holds. The corresponding line has been outstretched down to  $n_t = 0$ ; we call it border II. In an experiment where  $m_b$  is swept from zero to one at constant  $n_t = 0$  the transition between  $m = 0$  and  $m = 1$  occur at  $m_b = 0.5$  where border I is crossed. At finite temperature the transition is broadened in exactly the same way as for an isolated box (see highest peak in Fig. 2). The situation is quite different when  $n_t$  is held constant at  $n_t = 0.5$ .  $\bar{m}$  starts to increase as soon as  $m_b$  crosses border I and reaches

$\bar{m} = 1$  only when border II is reached (see the curve with discontinuities in Fig. 2). The distance of the two borders is given by  $\delta m = E_g/E_b$ . At finite temperature the discontinuities in  $d\bar{m}/dm_b$  are removed as shown by the broader peak in Fig. 2. If  $n_t$  is neither too close to 0 nor to 0.5, the electrometer current is a good measure of the box charge state. Fig. 4b shows the result of our six state approximation at zero temperature. As in the case of  $n_t = 0.5$  (Fig. 2) the transition from  $\bar{m} = 0$  to  $\bar{m} = 1$  occurs between the borders I and II. But for  $n_t < 0.5$  border II is less important than border I and vice versa at  $n_t > 0.5$ . At finite temperatures the discontinuities of Fig. 4b are removed, too.

The result for the sequential model is incorporated in Fig. 3 as lines. As in the experiment we have determined  $I_{sd}(m_b)$  for different values of  $n_t$  at varying temperatures. From  $I_{sd}(m_b)$  an effective temperature describing the width of the transition between neighboring box states can be deduced. The thick line in Fig. 3 corresponds to the average of  $T_{\text{eff}}$  over  $n_t$ . The thin lines correspond to the maximal and minimal  $T_{\text{eff}}$  found.

In summary we have shown that the coupling between a single-electron box and a single-electron electrometer which is used to measure the charge state of the box leads in general to a broadening of the transition between neighboring box states. The broadening only vanishes in cases where the electrometer has no sensitivity. This behavior is found in experiments as well as in the sequential model describing the system to lowest order in the dimensionless tunneling conductance  $g$ . However, the broadening found in our experiments exceeds the findings of the sequential model significantly suggesting that better agreement would be achieved by including higher order processes into the theoretical description.

We acknowledge fruitful discussions with G. Göppert, G. Johansson, H. v. Löhneysen and G. Schön.

\* Roland.Schaefer@ifp.fzk.de

† Fakultät für Physik, Universität Karlsruhe

- [1] P. Lafarge, H. Pothier, E. R. Williams, D. Esteve, C. Urbina, and M. H. Devoret, *Z. Phys. B - Condensed Matter* **85**, 327 (1991).
- [2] Y. Makhlin, G. Schön, and A. Shnirman, *Rev. Mod. Phys.* **73**, 357 (2001).
- [3] G. Johansson, A. Käck, and G. Wendin, *Phys. Rev. Lett.* **88**, 046802 (2002).
- [4] V. Bouchiat, D. Vion, P. Joyez, D. Esteve, and M. H. Devoret, *Physica Scripta* **T76**, 165 (1998).
- [5] G.-L. Ingold and Y. V. Nazarov, *Charge Tunneling Rates in Ultrasmall Junctions* (Plenum Press, New York, 1992), kapitel 2, no. Vol. 294 in NATO ASI series. Series B, Physics, ISBN 0-306-44229-9.
- [6] C. Wallisser, B. Limbach, P. vom Stein, R. Schäfer, C. Theis, G. Göppert, and H. Grabert, cond-mat/0205220.